A Novel Tube Lattice Slotted Core Highly Birefringent Photonic Crystal Fiber for THz Application

Animesh Bala,[a] Kanan Roy Chowdhury,[b,*] Md Borhan Mia,[a] Mohammad Faisal[a]
[a] Department of Electrical and Electronic Engineering, Bangladesh University of Engineering and Technology, Dhaka, Bangladesh
[b] Department of Electrical and Electronic Engineering, Chittagong University of Engineering and Technology, Chittagong, Bangladesh.

Abstract. A hexagonal slotted porous core tube lattice cladding photonic crystal fiber (SPC-TLC-PCF) is suggested to simultaneously achieve a very high birefringence and low transmission loss. At the operating frequency of 1 THz the proposed SPC-TLC-PCF yields a birefringence of 9.06×10−2 and effective material loss of 0.047 cm−1. The fiber operates at fundamental mode only and exhibits a small positive dispersion less than 1.6 ps/THz/cm over a band of 250 GHz (0.85 THz to 1.1 THz). Moreover, bending loss is around 1.61×10−7 cm−1 at 1 THz and confinement loss is also pretty small. These favorable attributes endorse this SPC-TLC-PCF much useful for polarization maintaining applications and sensing applications in THz regime.

Keywords: Photonic crystals, Fibers, Polarization-maintaining, Single-mode, Terahertz.

***** Correspondence Author**,** E-mail: u1502073@student.cuet.ac.bd.

1 Introduction

Electromagnetic radiation at terahertz (0.1–10THz) frequencies, located between microwaves and infrared rays, has attracted enormous attention of the researchers over the last few years due to its influential and promising applications in the fields of biotechnology,[1] spectroscopy,[2] imaging,[3] communication,[4] sensing,[5] medical diagnostics[6] etc. The three major steps of THz operation are generation, transmission and detection. Although the generation and detection techniques of THz wave have vastly improved, the real challenge lies in developing a suitable waveguide for the propagation at THz frequencies. To date, most of the THz system depends on wireless transmission since all the available materials cause serious absorption loss. Unfortunately, free space propagation has severe limitations, such as, large absorption by water vapor in the atmosphere, scattering loss by suspended particles, misalignment at the terminals, and complicated integration with other devices etc..[7,8] In order to overcome these problems, researchers employ their effort in designing different waveguides for THz wave propagation. For instance, metallic waveguides[9] were introduced, but they have huge bending loss and low coupling efficiency. Later, polyethylene as a guidance material[10] was introduced which has a low absorption loss. Furthermore, sub-wavelength air hole fiber,[11] polystyrene foam fiber,[12] hollow core Bragg fibers[13] were also proposed. In recent days, polymer fibers are vastly popular with material background such as Teflon[14], Plastic[15] and TOPAS©[16]. However, among these

TOPAS© is the most suitable one since it has a constant refractive index of n = 1.53 from 0.1 to 1.6 THz, which results in negligible material dispersion. Additionally, it is highly nonabsorbent of water vapor and has a very low bulk material absorption loss (0.2 cm^{-1}) at 1 THz.[17] Using these materials, solid core photonic crystal fibers (PCF) for THz wave transmission were proposed[14,18] which are disregarded due to large material loss. To solve this problem, porous core PCF with high air filling fraction at the core region is introduced[19] which offers comparatively low effective material loss.

The first porous core fiber was proposed by Atakaramians et al.[19] where the solid core is deliberately defected with smaller air holes, since dry air is assumed to have zero absorption loss and channeling most of the power through dry air leads to low effective material loss (EML). Later, the same group fabricated two types of porous core fibers[20] which also exhibit a birefringence of about 1.2×10^{-2} along with low absorption loss. High birefringence is an appealing property for polarization maintaining applications and photonic crystal fiber is an excellent candidate for achieving high birefringence in optical communication[21] and THz regime[22]. High birefringence can be achieved intentionally by creating asymmetry in the core and/or creating asymmetry in the cladding. Meanwhile, a squeezed lattice THz fiber is proposed by Chen et al.[23] with birefringence on the order of 10^{-2}. However, the squeezed design made the fabrication of this kind of fibers pretty difficult. In another design, Chen et al.[8] suggested a THz fiber with only elliptical air holes and obtained a birefringence of 4.45×10^{-2}. However, the effective material loss was 0.1 cm^{-1} which was not satisfactory, and the fabrication was also challenging. A novel design with a birefringence of 3.3×10^{-2} was proposed by Hasanuzzaman et al.[24] which contains only circular air holes but yields a high EML of 0.43 cm^{-1} at the operating frequency of 0.85THz. ecently, rectangular slots[25] were introduced in core region to achieve a higher birefringence value of 2.6×10^{-2}. Using the same technique, a THz fiber with a remarkable birefringence of 7.5×10^{-2} and low effective material loss of 0.07 cm^{-1} was reported by Islam et al..[26] A novel porous fiber based on dual-asymmetry is also introduced by Islam et al.[27] which shows birefringence value as high as 4.5×10^{-2} and effective absorption loss as low as 0.08 cm^{-1}. Hasan et al.[22] proposed a design which yields a high birefringence of 8.22×10^{-2} and a low EML of 0.05 cm^{-1}. This design is formed with slotted core kagome lattice cladding structure which is capable of providing very high birefringence along with a low EML. Meanwhile, a porous PCF is reported by Ahmed et al.[28] which shows birefringence in the order of 1.19×10^{-2} and an EML

of 0.0689 cm^{-1}. But the design contains elliptical air-holes which are difficult to fabricate, coupling efficiency reduces and the birefringence value is also low. Another recent design of porous core PCF proposed by Luo et al.[29] yields a high birefringence of 6.3×10^{-2} with an EML of 0.081 cm^{-1} at 1 THz. Though the features of this design are promising, both the birefringence and EML can be further improved.

In this paper, the main focus is to achieve an extremely high birefringence and therefore, a novel design with slotted porous core fiber is proposed. The reported design demonstrates a birefringence of 9.06×10^{-2} which is the highest at THz frequency regime till date. Moreover, the proposed PCF exhibits a low EML of 0.047 cm^{-1} for x-polarization mode following tube lattice cladding structure. The core diameters along with other parameters are optimized so that the highest birefringence is obtained. The fiber operates at fundamental mode only and the chromatic dispersion is less than 1.0 ps/THz/cm over a band of 250 GHz. Furthermore, other important properties such as power fraction, confinement loss, and bending loss are also investigated.

2 Design Methodology

The cross section of the proposed SPC-TLC-PCF is presented in Fig. 1. The core is hexagonal and the cladding is formed with tube lattice air-hole distribution. Air-slots are placed in the core region to introduce porosity, resulting in decrease in effective material loss. The asymmetric air-slots also introduce high birefringence. Cyclic olefin copolymer (COC) with a trade name of TOPAS© is selected as background material. No doping is introduced in the design to avoid extra cost and complexity in fabrication. The diameter of the slotted core is chosen as d_{core} = 320μm and the tube lattice cladding is formed with five rings of air-holes with a pitch of $\Lambda = d_{core}$ and diameter of $d = (d_{core} - w)$, where w is the distance between two adjacent air-holes. Throughout the design w = 10μm, which is kept constant so that the homogeneous material distribution aids the fabrication procedure. The central elongated hexagonal and two trapezoidal air-slots in both sides are placed such a way that the width of the hexagonal material boundary of the core region remains constant, w = 10 μm. The width of central elongated hexagonal air-slot is $w_0 = 0.1(d_{core} + w)$ and the width of two material slabs on either side of central elongated hexagonal air-slot is $w_1 = 0.15(d_{core} + w)$. All these parameters are illustrated in Fig. 1(b) to provide a precise idea. The porosity percentage, P in the core region can be calculated from following equation

$$P = \frac{\frac{3}{2}d^2 - 2w_1(2d - w_0 - w_1)}{\frac{3}{2}(d + 2w)^2} \times 100 \quad (1)$$

where Λ, d, w and w_0 are kept unchanged and only w_1 is altered to vary the porosity.

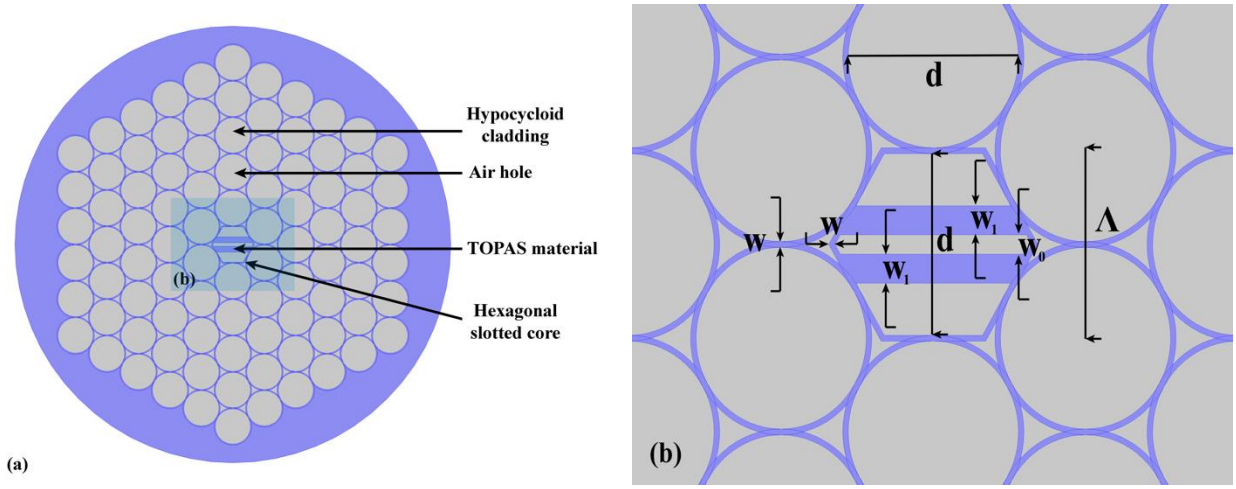

Fig.1 Transverse cross-section of the proposed PCF structure.

3 Simulations & Results

A full vector mode solver COMSOL Multiphysics 5.0 based on Finite Element Method (FEM) is used for numerical simulation to calculate various properties of the proposed PCF. A perfectly matched layer (PML) is positioned outside the computational domain as absorbing boundary in order to reduce the simulation window and to calculate the confinement loss. The simulation is performed for different core diameters and different core porosities while the frequency is varied from 0.5 to 1.1THz to get the highest birefringence value along with a well confined electric field at core region. The porosity is also controlled to achieve the lowest effective material loss (EML) as possible.

Fig. 2 presents the optical field distribution of x-polarization and y-polarization modes of the proposed SPC-TLC-PCF. It is evident from the figure that the mode field is well confined inside the core. The power fraction in different portions of the proposed PCF also endorses this feature. The power fraction η' can be calculated from following equation,[8]

$$\eta' = \frac{\int_{X} S_z \, dA}{\int_{All} S_z \, dA} \tag{2}$$

where $S_z = ½ \times \mathrm{Re}\,[E \times H^*]z$ is the Poynting vector towards the propagation direction of z. E and H are electric and magnetic fields, respectively and X denotes the area of interest for integration. Fig. 3 demonstrates the power flow in different parts of the proposed PCF. The calculation is carried out keeping the core diameter, $d_{core} = 320\mu m$.

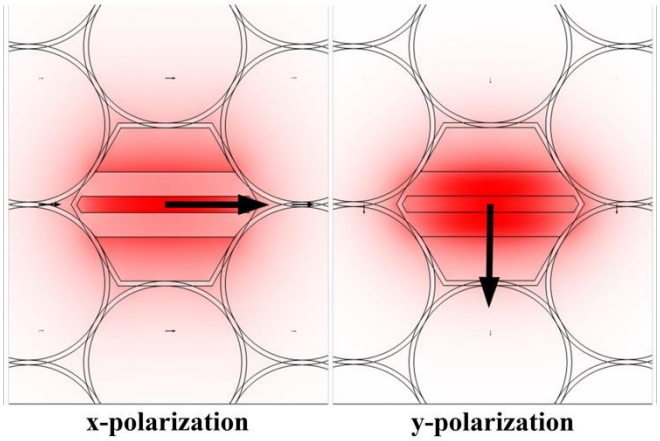

Fig. 2. Fundamental optical field distribution of the proposed PCF.

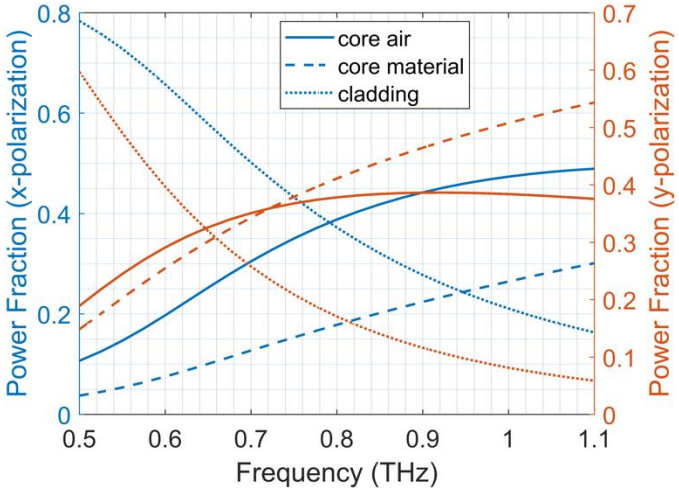

Fig. 3. Power fraction of the proposed PCF at different frequencies keeping $d_{core} = 320\mu m$ and porosity = 55%.

From Fig. 3 it is apparent that around 45% power flows through the air-core for x-polarization mode, whereas it is 43% for y-polarization mode at 1 THz. This ensures that a considerable amount of power propagates through air without experiencing material absorption.

The normalized frequency, i.e., the V-parameter is required to determine the single-mode guiding condition of a fiber. The value of V-parameter should remain less than 2.405 for fibers to be operated in single-mode which is a requisite to avoid intermodal dispersion. V-parameter can be calculated from following equation,[8]

$$V = \frac{2\pi rf}{\mathrm{c}} \sqrt{n_{co}^2 - n_{cl}^2} \leq 2.405 \tag{3}$$

where r is the effective radius of the core (= $d_{\mathrm{core}}/2$), c is the speed of light in vacuum, n_{co} and n_{cl} are refractive indices of the fiber core and cladding, respectively. In case of our proposed SPC-TLC-PCF, the cladding is mostly formed with dry air. Therefore, refractive index of cladding is calculated as $n_{cl} \approx \sqrt{F + (1-F)n_s^2}$,[30] where F is the air filling fraction and n_{s} is the refractive index of the host material. The core's refractive index, n_{co} is regarded as effective mode index n_{eff} of the fiber, which is calculated from simulation. Fig. 4 demonstrates the V-parameter of the proposed PCF for both x and y-polarization modes at different porosities. The porosity is varied by varying the width of two material slabs (w_1) on either side of central elongated hexagonal air-slot in core. For 55%, 45% and 35% porosities, w_1 is calculated as $w_{1(P\,=\,55\%)} = 0.15(d_{\mathrm{core}} + w)$, $w_{1(P\,=\,45\%)} = 0.2(d_{\mathrm{core}} + w)$ and $w_{1(P\,=\,35\%)} = 0.25(d_{\mathrm{core}} + w)$, respectively. From Fig. 4 it is obvious that the proposed SPC-TLC-PCF operates at fundamental mode only within a certain range of core diameter. At 1THz, for 55%, 45% and 35% porosity the fiber operates at fundamental mode below the core diameter value of 338μm, 311μm and 295μm, respectively.

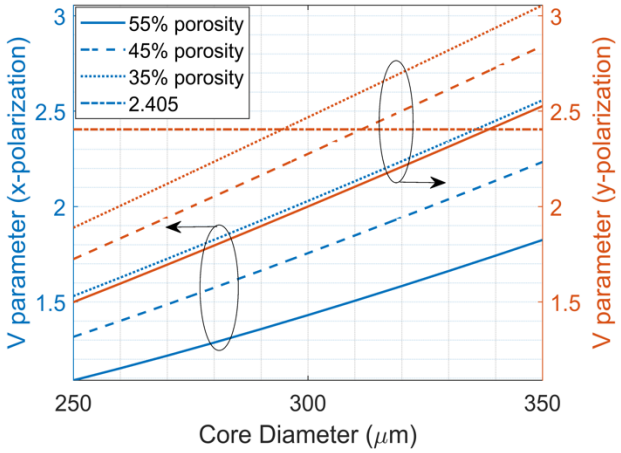

Fig. 4. V-parameter of x and y-polarization modes of the proposed PCF as a function of core diameters.

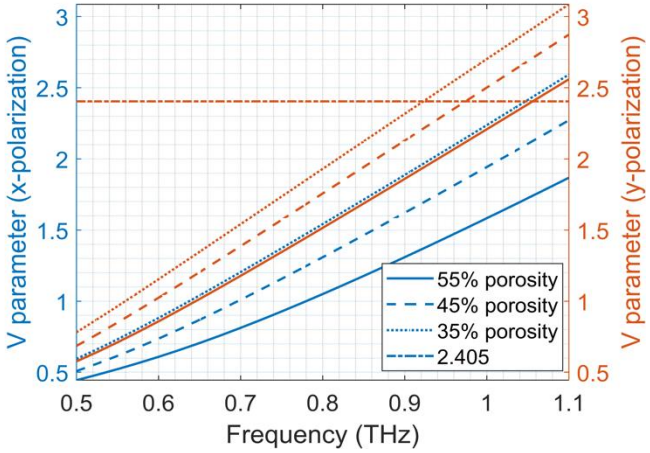

Fig. 5. V-parameter of x and y-polarization modes of the proposed PCF as a function of operating frequency.

Fig. 5 displays the variation of V-parameter for both degenerate modes as a function of operating frequency. The curves are plotted for different porosities and core diameter of 320 μm. It has been observed that for different porosity values, fundamental mode sustains up to different frequencies. It is also evident that highest range of frequency can be achieved when porosity is 55%, over which the proposed fiber operates at fundamental mode only.

The birefringence of the proposed PCF is presented in Fig. 6 for different core diameters and porosities. The birefringence can be calculated using the following equation,

$$B = \left| n_x - n_y \right| \tag{4}$$

where n_x and n_y are the effective mode index of x-polarization and y-polarization modes, respectively. While the core diameter is increased, the slot size in the core also increases, resulting in the increment of asymmetry in the core region. This leads to the rise in birefringence value. Moreover, increment of porosity leads to decrement of slot width, resulting in increment of inhomogeneous material distribution along x and y direction. This increases asymmetry between x and y-polarized mode fields; therefore, increases birefringence.

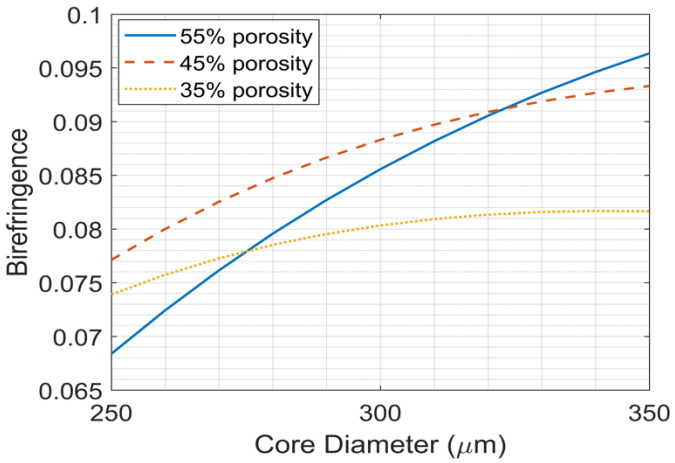

Fig. 6. Birefringence of the proposed PCF for different core diameters and porosities.

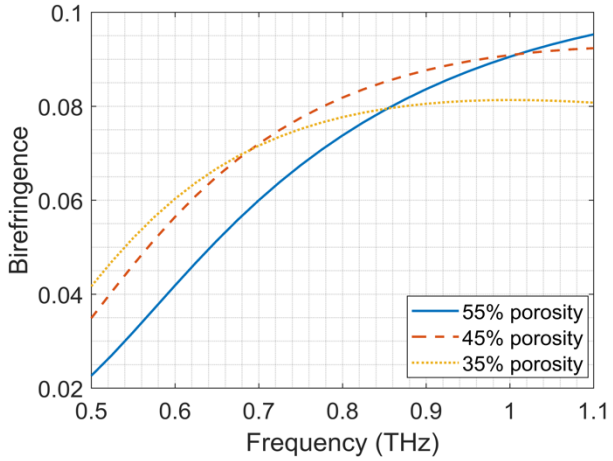

Fig. 7. Birefringence of the proposed PCF at different frequencies when d_{core} is 320μm.

Although the increment of core diameter enhances the birefringence, from Fig. 4 it is clear that, the core diameter should be kept less than a distinct value to operate the fiber at fundamental mode only. At 55% porosity and core diameter of 320μm, the single mode sustains up to about 1.1THz. Keeping this in concern, the highest birefringence value of 9.06×10^{-2} can be achieved conveniently at 1THz frequency. At this point, w = 10μm, w_0 = 33μm, w_1 = 49.5μm, Λ = 320μm and d = 310μm. Fig. 7 presents the birefringence property of the proposed PCF as a function of frequency for these optimum parameters. Since at higher frequencies, mode field confinement towards the core arises, asymmetry between the two fundamental degenerate mode fields increases, resulting in the increment of birefringence value.

In THz communication, three major losses needed to be considered are effective material loss (EML), confinement loss and bending loss. The EML or the absorption loss is the most crucial parameter to be regarded, as it is mainly responsible for limiting THz transmission. EML can be calculated using the following expression obtained by perturbation theory.[8]

$$\alpha_{eff} = \sqrt{\frac{\varepsilon_0}{\mu_0}} \frac{\int_{A_{mat}} n\alpha_{mat} |E|^2 dA}{2\int_{All} S_z dA} = \alpha_{mat}\eta \tag{5}$$

where ε_0 and μ_0 are the permittivity and the permeability of the vacuum, respectively. Fig.8 represents the EML as a function of frequency at different porosities. The figure depicts that EML decreases with the increase of porosity. This is because with the increase of porosity more optical power passes through dry air resulting in less interaction with material and reduction of material absorption loss. Furthermore, EML increases with the operating frequency due to the increment of mode field concentration at core region. At 1 THz, EML is found 0.047 cm^{-1} for x-polarization mode with 55% porosity which is much lower.

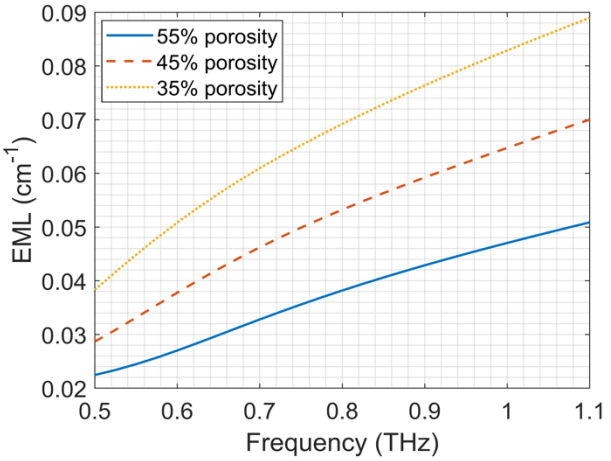

Fig. 8. EML as a function of frequency at different porosities when d_{core} is 320μm.

Confinement is another loss associated with PCF, which occurs due to the finite range of cladding and can be calculated from the following expression, [31]

$$\alpha_{CL} = 8.686 k_0 \, \mathrm{Im}(n_{eff}) \tag{6}$$

where Im(n_{eff}) is the imaginary part of the refractive index of the guided mode and $k_0 = 2\pi/\lambda$. In Fig. 9, confinement loss is plotted as a function of frequency for two polarization modes. For both polarization modes, confinement loss decreases with the increment of frequency, since at higher frequencies mode field tends to be more confined in the core. The confinement loss of x-polarization mode is higher than that of y-polarization mode due to the less confinement of field along x direction, which is due to the asymmetric slots and inhomogeneous material distribution at core. It is noteworthy that at 1 THz the confinement loss is 6.815×10^{-7} cm^{-1} for x-polarization mode and 9.093×10^{-12} cm^{-1} for y-polarization mode.

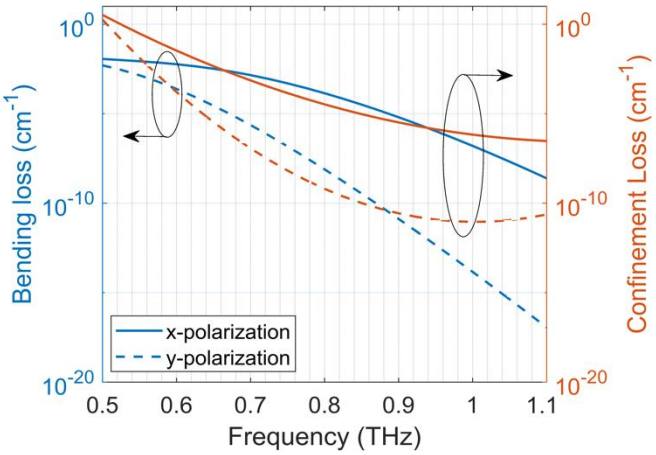

Fig. 9. Confinement loss and bending of the proposed PCF at different frequencies keeping d_{core} = 320μm and porosity = 55%.

While using fibers, bending of the fibers is a common occurrence. Bending leads to a loss in fiber which can be calculated by the following equation,[11]

$$\alpha_{BL} \approx \frac{1}{8}\sqrt{\frac{2\pi}{3}}\frac{1}{A_{eff}}\frac{1}{\beta}\mathrm{F}\left[\frac{2}{3}R\frac{\left(\beta^2-\beta_{cl}^2\right)^{\frac{3}{2}}}{\beta^2}\right] \tag{7}$$

where R is the bending radius, $F(x) = x^{-1/2} e^{-x}$, $\beta = 2\pi n_{eff}/\lambda$ is the propagation constant and A_{eff} is the effective area expressed as,[31]

$$A_{eff} = \left[\int I(r)rdr\right]^2\left[\int I^2(r)rdr\right]^{-1} \tag{8}$$

where $I(r)=|E|^2$ is the transverse electric field intensity distribution in the fiber cross section. Fig. 9 also demonstrates the bending loss of the proposed SPC-TLC-PCF at different frequencies. The bending radius is considered as R = 1 cm for calculation. In case of our proposed design, bending losses are less than 10^{-10} cm^{-1} for both x and y-polarization modes, which are very small for PCFs at THz regime.

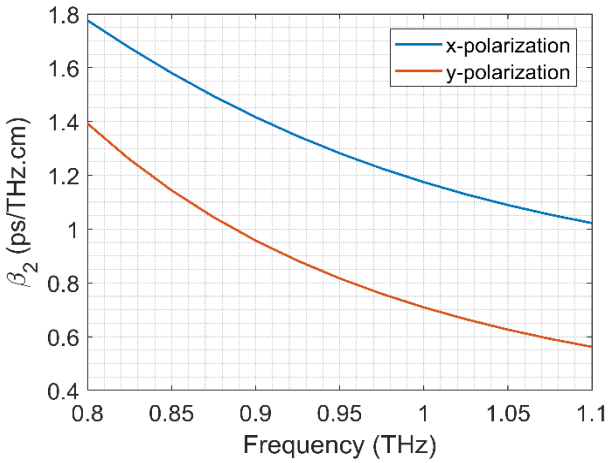

Fig. 10. Chromatic dispersion of the proposed PCF keeping d_{core} = 320μm and porosity = 55%.

As fibers in THz regime (0.2-1.5THz) are fabricated with TOPAS© material which has a constant refractive index, the material dispersion is negligible for these fibers. However, the waveguide dispersion should be kept in consideration. The total chromatic dispersion can be calculated by following equation in frequency domain,[32]

$$\beta_2 = \frac{2}{c}\frac{dn_{eff}}{d\omega} + \frac{\omega}{c}\frac{d^2 n_{eff}}{d\omega^2} \tag{9}$$

where $\omega = 2\pi f$ is the angular frequency where f is the frequency. From Fig. 10, it is evident that the dispersion is very small for our proposed SPC-TLC-PCF. The dispersion is less than 1.5 ps/THz/cm and 1.0 ps/THz/cm over a band of 200 GHz (0.9 THz to 1.1 THz) for x- and y-polarization modes, respectively. This small dispersion ensures very little broadening of propagating pulses through the fiber.

Table 1: Core diameter and slab width variation of the proposed PCF.

Core diameter variation (keeping other parameters fixed)					
Variation	-10%	-5%	0%	+5%	+10%
B ($\times 10^{-2}$)	8.21	8.66	9.06	9.39	9.67
EML(cm^{-1})	0.0445	0.0456	0.047	0.0483	0.0497

Slab width variation (keeping other parameters fixed)					
Variation	-10%	-5%	0%	+5%	+10%
B ($\times10^{-2}$)	8.63	8.9	9.06	9.17	9.29
EML(cm^{-1})	0.0424	0.0448	0.047	0.0493	0.052

Table 1 has depicted the values of birefringence and EML due to ±5% and ±10% deviation from the optimum core diameter and slab width considering the issue that the fabricated fiber can deviate from the proposed one. During slab width variation, both the slabs are varied equally. It is observed that a −10% variation of core diameter results in a birefringence of 8.21×10^{-2} which is low from the proposed design but still pretty high. On the other hand, a 10% reduction in slab width results in a birefringence of 8.63×10^{-2} which is approximately 4% less than the proposed fiber. Moreover, no significant change in EML has been observed in both core diameter and slab width variation.

Table 2: Comparison of the proposed PCF with other reported designs.

Ref	B $\times10^{-2}$	EML (cm^{-1})	α_{CL} (cm^{-1})	α_{BL} (cm^{-1})	β_2 ps/THz/cm
[8]	4.45	0.1	-	-	-
[22]	8.22	0.05	4.13×10^{-5}	-	0.57
[26]	7.5	0.07	0.3	-	1.5
[27]	4.5	0.08	-	0.01	-
[28]	1.19	0.068	-	-	-
[33]	6.22	0.6	-	-	-
[34]	1.05	0.07	0.1	0.2	2.92
SPC-TLC PCF	9.06	0.047	6.81×10^{-7}	1.61×10^{-7}	1.17

Table 2 represents the comparisons among the birefringence (*B*), EML, confinement loss (α_{CL}) and bending loss (α_{BL}) and dispersion (β_2) of the proposed design with some recent prior works at 1 THz. From the table, it is evident that the proposed fiber produces the highest birefringence than any other previously reported designs. The value of EML of the proposed SPC-TLC-PCF is 0.047 cm^{-1} whereas the highest birefringence value among previous works close to our work yields EML of 0.05 cm^{-1}. Furthermore, confinement loss, bending loss and chromatic dispersion also

exhibits much lower value than the other designs.

Lastly, fiber fabrication is an important issue to consider while designing a fiber. The proposed fiber consists of a slotted core while maintaining a periodic circular tube lattice through its cladding. Fibers with tube lattice and hypocycloid cladding are already being fabricated.[35-37] Another similar type of high air filling fraction and homogeneous material distributed cladding kagome lattice structure has also been fabricated by Argyros *et al*..[38] Furthermore, the extrusion technique developed by Kiang *et al*.[39] for non-silica fiber allows great design flexibility which can be used to extrude the slotted core of the proposed fiber. Moreover, to ease the fabrication, the sharp edges of the hexagonal core can be smoothed using fillet. When the fillet radius is about 5% of the core diameter, the fiber shows a birefringence value of 8.8×10^{-2} which is still pretty high.

4. Conclusion

In this paper, a highly birefringent slotted core THz fiber is reported. Tube lattice cladding is used to keep the EML as low as possible. The designed fiber demonstrates a very high birefringence of 9.06×10^{-2} and an EML of 0.047 cm^{-1} with a very low confinement loss. The fiber also demonstrates pretty small bending loss and low dispersion over a band of 250 GHz. Considering the fabrication feasibility and all these optical properties, the proposed SPC-TLC-PCF can be an excellent candidate in the field of THz application where polarization preservation is a significant issue.

References:

1. Emiliyanov, G., Jensen, J. B., Bang, O. *et al.* (2007): "Localized biosensing with Topas microstructured polymer optical fiber," *Opt. Lett.*, 32, 5, p. 460-462.
2. Han, P.Y., Tani, M., Usami, M., Kono, S., Kersting, R. and Zhang, X.C. (2001): "A direct comparison between terahertz time-domain spectroscopy and far-infrared Fourier transform spectroscopy," *J. Appl. Phys.*, 89, 4, pp. 2357–2359.
3. Fukunaga, K., Sekine, N., Hosako, I., Oda, N., Yoneyama, H. and Sudoh, T. (2008): "Real-time terahertz imaging for art conservation science," *J. Eur. Opt. Soc. Rapid Publ.*, 3, 0, pp. 8027-8030.
4. Möller, L., Federici, J., Sinyukov, A., Xie, C., Lim, H.C. and Giles, R.C. (2008): "Data encoding on terahertz signals for communication and sensing," *Opt. Lett.*, 33, 4, p. 393-396.
5. Yuan, W., Khan, L., Webb, D.J. *et al.* (2011): "Humidity insensitive TOPAS polymer fiber Bragg grating sensor," *Opt. Express*, 2011, 19, 20, pp. 19731-19739.
6. Woodward, R. M., Wallace, V. P., Arnone, D. D., Linfield, E. H. and Pepper, M. (2003): "Terahertz Pulsed Imaging of Skin Cancer in the Time and Frequency Domain," *J. Biol. Phys.*, 29, 2/3, pp. 257–259.
7. Yang, Y. (2014): "Atmospheric Effects on Free-Space THz," *J. Lasers, Opt. Photonics*, 1, 2, pp. 1–2.
8. Chen, N., Liang, J. and Ren, L. (2013): "High-birefringence, low-loss porous fiber for single-mode terahertz-wave guidance," *Appl. Opt.*, 52, 21, pp. 5297-5301.
9. Wang, K. and Mittleman, D. M. (2004): "Metal wires for terahertz wave guiding," *Nature*, 432, 7015, pp. 376–379.
10. Chen, L.J., Chen, H.W., Kao, T.F., Lu, J.Y. and Sun, C.K. (2006): "Low-loss subwavelength plastic fiber for terahertz waveguiding," *Opt. Lett.*, 31, 3, pp. 308-312.
11. Hassani, A., Dupuis, A. and Skorobogatiy, M. (2008): "Low loss porous terahertz fibers containing multiple subwavelength holes," *Appl. Phys. Lett.*, 92, 7, pp. 71101.
12. Zhao, G., Mors, M.T., Wenckebach, T. and Planken, P. C. M. (2002): "Terahertz dielectric properties of polystyrene foam," *J. Opt. Soc. Am. B*, 19, 6, pp. 1476.

13. Vincetti, L. (2009):"Numerical analysis of plastic hollow core microstructured fiber for Terahertz applications," *Opt. Fiber Technol.*, 15, 4, pp. 398–401.
14. Goto, M., Quema, A., Takahashi, H., Ono, S. and Sarukura, N. (2004): "Teflon Photonic Crystal Fiber as Terahertz Waveguide," *Jpn. J. Appl. Phys.*, 43, 2B, pp. L317–L319.
15. Vincetti, L. (2009): "Hollow core photonic band gap fiber for THz applications," *Microw. Opt. Technol. Lett.*, 51, 7, pp. 1711–1714.
16. Zhu, Y. F., Chen, M.Y., Wang, H., Yao, H.B. Zhang, Y.K.and Yang, J.C. (2013):"Design and Analysis of a Low-Loss Suspended Core Terahertz Fiber and Its Application to Polarization Splitter," *IEEE Photonics J.*, 5, 6, pp. 7101410–7101410.
17. Atakaramians, S., Afshar, S., Monro, V.T.M. and Abbott, D. (2013): "Terahertz dielectric waveguides," *Adv. Opt. Photonics*, 5, 2, pp. 169
18. Han, H., Park, H., Cho, M. and Kim, J. (2002): "Terahertz pulse propagation in a plastic photonic crystal fiber," *Appl. Phys. Lett.*, 80, 15, pp. 2634–2636.
19. Atakaramians, S., Afshar S., Fischer, V, B. M., Abbott, D. and Monro, T.M. (2008): "Porous fibers: a novel approach to low loss THz waveguides." *Opt. Express*, 16, 12, pp. 8845–8854.
20. Atakaramians, S., Afshar, S., Heidepriem, H.E. *et al*.(2009):"THz porous fibers: design, fabrication and experimental characterization," *Opt. Express*, 17, 16, pp. 14053-14062.
21. Bala, A., Chowdhury, K.R., Mia, M.B. and Faisal, M. (2017): "Highly birefringent, highly negative dispersion compensating photonic crystal fiber," *Appl. Opt.*, 56, 25, pp. 7256-7262.
22. Hasan, M.R., Anower, M.S., Hasan, M.I. and Razzak, S.M.A. (2016): "Polarization Maintaining Low-Loss Slotted Core Kagome Lattice THz Fiber," *IEEE Photonics Technol. Lett.*, 28, 16, pp. 1751–1754.
23. Chen, H., Chen, D. and Hong, Z. (2009): "Squeezed lattice elliptical-hole terahertz fiber with high birefringence," *Appl. Opt.*, 48, 20, pp. 3943-3949.
24. Hasanuzzaman, G. K. M., Rana, S. and Habib, M.S. (2016): "A Novel Low Loss, Highly Birefringent Photonic Crystal Fiber in THz Regime," *IEEE Photonics Technol. Lett.*, 28, 8, pp. 899–902.

25. Atakaramians, S., Afshar, S., Fischer, V.B.M., Abbott, D. and Monro, T.M. (2005): "Low loss, low dispersion and highly birefringent terahertz porous fibers," *Opt. Commun.*, 282, 1, pp. 36–38.
26. Islam, R., Habib, S. M., Hasanuzzaman, G.K.M., Rana, S. and Kaijage, S.F.(2015): "Extremely High-Birefringent Asymmetric Slotted-Core Photonic Crystal Fiber in THz Regime," *IEEE Photonics Technol. Lett.*, 27, 21, pp. 2222–2225.
27. Islam, R., Habib, S. M., Hasanuzzaman, G.K.M., Rana, S. and Sadath, M.A.(2016): "Novel porous fiber based on dual-asymmetry for low-loss polarization maintaining THz wave guidance," *Opt. Lett.*, 41, 3, pp. 440–443.
28. Ahmed, K., Chowdhury, S., Paul, B. K. *et al.*(2017): "Ultrahigh birefringence, ultralow material loss porous core single-mode fiber for terahertz wave guidance," *Appl. Opt.*, 56, 12, pp. 3477-3483.
29. Luo, J., Tian, F., Qu, H. *et al.*(2017): 'Design and numerical analysis of a THz square porous-core photonic crystal fiber for low flattened dispersion, ultrahigh birefringence', *Appl. Opt.*, 56, 24, pp. 6993-7001.
30. Islam, M. S., Faisal, M. and Razzak, S. M. A. (2017): 'Extremely Low Loss Porous-Core Photonic Crystal Fiber with Ultra Flat Dispersion in THz Regime', *JOSA B,* 34, 8, pp. 1747-1754.
31. [31]Kaijage, S. F., Ouyang, Z. and Jin, X. (2013): 'Porous-Core Photonic Crystal Fiber for Low Loss Terahertz Wave Guiding', *IEEE Photonics Technol. Lett.*, 25, 15, pp. 1454–1457.
32. Liang, J.,Ren, L., Chen, N. and Zhou, C. (2013): 'Broadband, low-loss, dispersion flattened porous-core photonic bandgap fiber for terahertz (THz)-wave propagation', *Opt. Commun.*, 295, pp. 257–261.
33. Chen, H., Wang, J. and Shi, W. (2014): 'A High Birefringent Polymer Terahertz Waveguide: Suspended Elliptical Core Fiber', *J. Opt. Soc. Korea, 18, 5, pp. 453-458,* vol. 18, no. 5, pp. 453–458.
34. Islam, R., Habib, M. S., Hasanuzzaman, G. K. M., Rana, S., Sadath, M. A. and Markos, C. (2016): 'A Novel Low-Loss Diamond-Core Porous Fiber for Polarization Maintaining Terahertz Transmission', *IEEE Photonics Technol. Lett.*, 28, 14, pp. 1537–1540.

35. Lu, W., Lou, S. and Argyros, A. (2016): 'Investigation of Flexible Low-Loss Hollow-Core Fibres With Tube-Lattice Cladding for Terahertz Radiation', *IEEE J. Sel. Top. Quantum Electron.*, 22, 2, pp. 214–220.
36. Debord, B., Alharbi, M., Bradley, T., *et al.* (2013): 'Hypocycloid-shaped hollow-core photonic crystal fiber Part I: Arc curvature effect on confinement loss', *Opt. Express*, 21, 23, pp. 28597-28608.
37. Setti, V., Vincetti, L. and Argyros, A. (2013): 'Flexible tube lattice fibers for terahertz applications', *Opt. Express*, 21, 3, pp. 3388.
38. Argyros, A. and Pla, J. (2007): 'Hollow-core polymer fibres with a kagome lattice: potential for transmission in the infrared', *Opt. Express*, 15, 12, pp. 7713–7719.
39. Kiang, K. M., Frampton, K., Morno, M., *et al.*(2002): 'Extruded singlemode non-silica glass holey optical fibres', *Electron. Lett.*, 38, 12, pp. 546-547.

